OPEN ACCESS
IOP Publishing
Journal of Physics A: Mathematical and Theoretical
J. Phys. A: Math. Theor. **58** (2025) 025209 (14pp)
https://doi.org/10.1088/1751-8121/ada0fb

Efficient evaluation of lattice Green's functions

Andriy Zhugayevych

Max Planck Institute for Polymer Research, Ackermannweg 10, 55128 Mainz, Germany

E-mail: andriy.zhugayevych@mpip-mainz.mpg.de

Received 11 May 2024; revised 30 November 2024
Accepted for publication 18 December 2024
Published 27 December 2024

Abstract

We develop and implement efficient algorithms for calculating lattice Green's functions (LGFs) at any point and argument. This includes several approaches: recurrence relations in lattice coordinates, series at zero and infinity, and finite-precision uniform approximations. The methodology can be applied to any simple lattice, whereas program code is provided for triangular and hypercubic lattices. In particular, the obtained generic recurrence relations are applicable to any lattice with a root-free band dispersion. Except for lattices with a high coordination number, these relations allow LGF to be presented as a linear combination of d non-polynomial functions with polynomial coefficients, where d is the lattice dimension. The non-polynomial functions are solutions of d-order differential equation with polynomial coefficients which allows their series expansion at singularities to be performed. For series at infinity, we estimate the remainder, thus extending its use to the zero value of the argument. The remainder itself provides a good finite-precision estimate for the LGF. Finally, we derive a large-scale approximation that smoothly connects the lattice and the continuum Green's functions. The provided open-source code allows for arbitrary-precision and symbolic computations of LGF.

Supplementary material for this article is available online

Keywords: lattice Green's function, hypercubic lattice, lattice models, special functions, random walk

1. Introduction

Lattice Green's function (LGF) is the resolvent of the lattice Laplacian. For simplicity, we consider primitive lattices, so that all points are translationally equivalent and thus

$$g_{xy}(s) = \left[(s-\Delta)^{-1}\right]_{xy} \equiv g_{x-y}(s), \tag{1}$$

where the coordinates $x, y \in \mathbb{Z}^d$ enumerate lattice points, d is the lattice dimension, and the argument $s \in \mathbb{C}$. LGF is commonly utilized for solving quantum and statistical lattice models with a nearest-neighbor interaction [1–4]. In such applications, the mean-field solution is given by a rescaled LGF, and correlation corrections involve the summation of the LGF over the lattice, thus requiring an efficient algorithm for its evaluation. Formally, any LGF can be calculated using the Fourier integral:

$$g_x(s) = \frac{1}{(2\pi)^d} \int \cdots \int_{-\pi}^{\pi} \frac{\mathrm{e}^{-\mathrm{i}kx}}{s - S(k)}\, \mathrm{d}k, \tag{2}$$

where $kx = \sum_{i=1}^{d} k_i x_i$ in lattice coordinates,

$$S(k) = \sum_{|z|=1} (\cos kz - 1) \tag{3}$$

is the band dispersion, and $|z|$ is the shortest-path distance (the smallest number of steps between the origin and the lattice point z). However, this approach is impractical at singular points owing to the zero denominator and for large values of coordinates because of the highly oscillating numerator requiring ultrafine integration grids [5]. Therefore, a number of other approaches have been developed allowing for an arbitrary-precision evaluation of the LGF for any argument. In particular, $g_0(0)$ for cubic lattices was reduced to known special functions almost a century ago [6, 7]. Efficient algorithms for simple two-dimensional lattices were developed in the 1970s [8–10]. Proof-of-principle results for three-dimensional lattices were also obtained in that period [11, 12], but computationally efficient formulas in terms of elliptic integrals were derived much later [13]. Multidimensional lattices are less studied, although numerous identities are known [1], including series at zero for hypercubic lattice [14]. All these results suggest finding generic approaches for the efficient and easy-to-implement evaluation of LGF, at least for simple lattices, which is the ultimate goal of the present work.

To summarize the current state of the art in LGF evaluation, we note that there are several basic complementary approaches illustrated in figure 1. Universally applicable are Fourier integrals and path expansion series. The latter can be defined as the perturbation expansion of the resolvent in off-diagonal elements such that for a lattice of identical sites

$$g_x(s) = \sum_{n=0}^{\infty} \frac{N_x(n)}{(s+w)^{n+1+|x|}}, \tag{4}$$

where $N_x(n)$ are some coefficients implicitly dependent on the free parameter w which can be conveniently chosen to simplify the coefficients N. If w is the lattice coordination number, then $N_x(n)$ is the number of paths of the length $n+|x|$. For simple lattices, explicit formulas for N are available and can be efficiently evaluated recursively in d [15]. Missing is a series remainder: because all terms in equation (4) are positive, by estimating the remainder we can

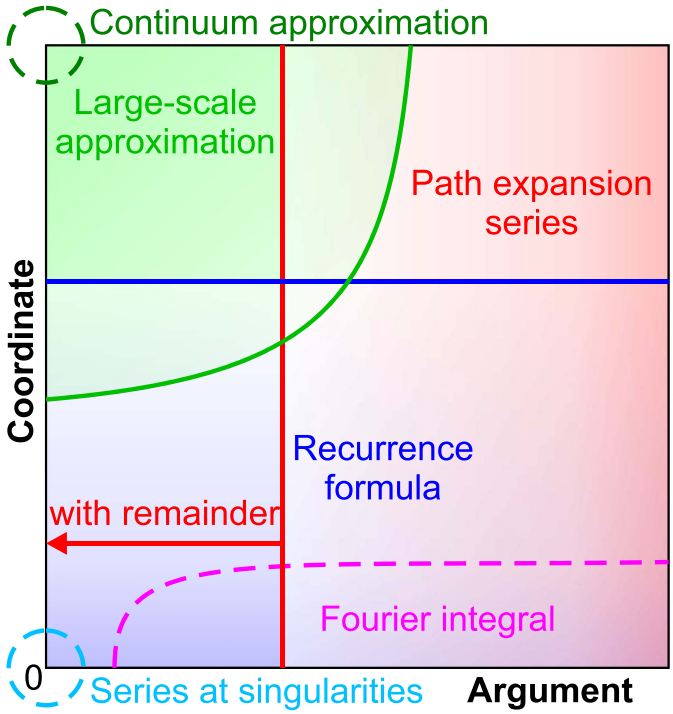

Figure 1. Schematic overview of LGF evaluation methods showing the range of their applicability. On this and other figures the argument in $g_x(s)$ is positive. The 'coordinate' here means either components of x or its norm such as $|x|$ or $\|x\|$. The scale of both axes is unit.

obtain upper and lower boundaries for the LGF, make equation (4) usable even for $s=0$, and provide uniform approximation for the LGF. Another common approach relies on the existence of one-dimensional recurrence relations in coordinates allowing to present the LGF at any point as a linear combination of the LGF at a seeding set of points, which we call the LGF basis. Such relations do exist for all simple two- and three-dimensional lattices. The basis functions must be evaluated by other methods. For large s it can be performed by the path expansion series, whereas small s requires series expansion at zero. The latter can usually be obtained from a linear differential equation for g_0 which is known for many lattices [1]. Therefore, it is reasonable to expect the existence of generic recurrence relations and differential equations for LGF for any simple lattice. All the approaches discussed thus far are inefficient in the large-scale region (small s and large x). Here the Green's function of the Laplacian in $\mathbb{R}^d$ can be used as a zero-order approximation, but corrections are needed to smoothly connect it to the LGF. The aim of the present work is to provide all the aforementioned missing formulas and implement all the discussed above approaches in an efficient program code for triangular and hypercubic lattices representing two archetypal classes of simple lattices.

The manuscript is organized as follows, with the approaches presented in the order from universal to lattice-specific. First, we derive the large-scale approximation. We then obtain the path expansion series remainders. Next, we derive generic recurrence relations in the coordinates and differential equations for LGF. Finally, we briefly outline the construction of the series expansion at zero. All the generic methods are illustrated for hypercubic and triangular lattices.

Complete derivations, technical details, implementation, code and its documentation are published on the project webpage at https://cmsos.github.io/lgf/.

2. Large-scale approximation

At large scales, the Green's function of any regular lattice tends to the resolvent of Laplacian in $\mathbb{R}^d$ which is

$$g(s,x) = \frac{1}{(2\pi)^{d/2}} \left(\frac{\sqrt{s}}{\|x\|}\right)^{\frac{d}{2}-1} K_{\frac{d}{2}-1}\left(\sqrt{s}\|x\|\right), \tag{5}$$

where K is the modified Bessel function of the second kind and $\|x\|$ is the Euclidean distance for the lattice embedded in $\mathbb{R}^d$ with the unit bond (edge) length. The inverse Laplace transformation of this function is the propagator of the diffusion equation:

$$\tilde{g}(t,x) = \frac{1}{2\pi\mathrm{i}} \int_{-\mathrm{i}\infty}^{+\mathrm{i}\infty} g(s,x)\, \mathrm{e}^{st}\, \mathrm{d}s = \frac{1}{(4\pi t)^{d/2}} \exp\left(-\frac{\|x\|^2}{4t}\right). \tag{6}$$

To approximate LGF by equation (6), the latter must be properly rescaled as

$$\tilde{g}^{\mathrm{lat}}(t,x) = \frac{V_1}{(4\pi Dt)^{d/2}} \exp\left(-\frac{\|x\|^2}{4Dt}\right), \tag{7}$$

where V_1 is the volume per lattice point, $D = w_0/(2d)$ is the diffusion constant and w_0 is the lattice coordination number. For the hypercubic lattice, both V_1 and D are unit, whereas for the triangular lattice $V_1 = \sqrt{3}/2$ and $D = 3/2$.

A more accurate description can be obtained using large-scale approximation. We derive it for propagators and then perform a Laplace transformation of the result. The propagator of equation (2) is

$$\tilde{g}_x(t) = \frac{1}{(2\pi)^d} \int \cdots \int_{-\pi}^{\pi} \mathrm{e}^{tS(k)-\mathrm{i}kx}\, \mathrm{d}k. \tag{8}$$

At large t and x, this integral can be calculated using the saddle-point method. The saddle point of the exponent is at $k = -\mathrm{i}\kappa$, where $\kappa \equiv \kappa(t)$ is a solution to the equations

$$\frac{\partial \tilde{S}}{\partial \kappa_i} = \frac{x_i}{t},\ i = 1,\ldots,d, \quad \text{where } \tilde{S}(\kappa) = S(-\mathrm{i}\kappa). \tag{9}$$

When the integration path in equation (8) is shifted by $-\mathrm{i}\kappa$, the integrand has a sharp maximum at zero and reduced oscillations on the path, such that the integral can be approximated by the Gaussian integral:

$$\tilde{g}_x(t) = \frac{1}{(2\pi)^d} \int \cdots \int_{-\pi}^{\pi} \mathrm{e}^{tS(k-\mathrm{i}\kappa)-\kappa x-\mathrm{i}kx}\, \mathrm{d}k \approx \frac{\mathrm{e}^{t\tilde{S}(\kappa)-\kappa x}}{\sqrt{\det 2\pi t\tilde{S}''(\kappa)}}, \tag{10}$$

where $\tilde{S}''$ is Hessian. If $t \to \infty$, $\kappa \to 0$ and $\tilde{S}(\kappa) \sim \kappa^2$ yielding $\kappa \sim x/t$ thus recovering the continuum Green's function (7).

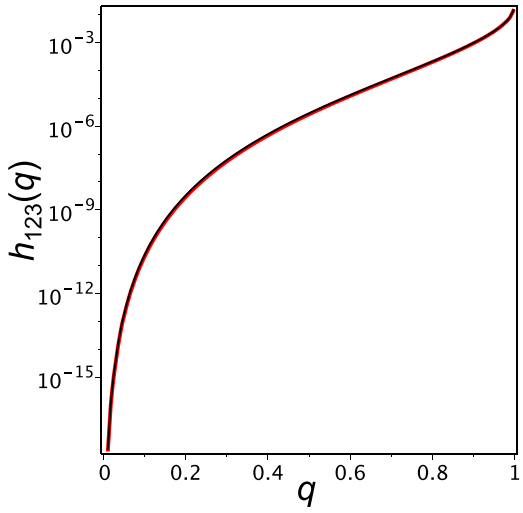

Figure 2. Large-scale approximation (red curve versus exact-LGF black curve) for simple cubic lattice is accurate even for small values of coordinates, $x = (1,2,3)$. The argument q is defined by equation (14).

The Laplace transformation of equation (10) can be performed only approximately by the quadratic expansion of the exponent at the integrand's maximum (a variant of the saddle-point method) yielding:

$$g_x(s) \approx \sqrt{\frac{2\pi}{-\ddot{\tilde{S}}}}\,\frac{\mathrm{e}^{-\kappa x}}{\sqrt{\det 2\pi t\tilde{S}''}} \tag{11}$$

with the equation $\tilde{S}(\kappa(t)) = s$ for t, where the dot indicates the time derivative, the argument of $\tilde{S}$ is omitted for clarity, and

$$-\ddot{\tilde{S}} \equiv -\frac{\dot{\kappa}x}{t} \equiv t\sum_{i,j=1}^{d} \tilde{S}''_{ij}\dot{\kappa}_i\dot{\kappa}_j, \text{ so that } \dot{\kappa} = -\frac{\left(\tilde{S}''\right)^{-1}x}{t^2}. \tag{12}$$

For small s

$$t = \frac{\|x\|}{2\sqrt{s}} \Longrightarrow g_x(s) \approx \frac{1}{2\sqrt{s}}\left(\frac{\sqrt{s}}{2\pi\|x\|}\right)^{\frac{d-1}{2}} \mathrm{e}^{-\|x\|\sqrt{s}}. \tag{13}$$

Owing to the additional approximations made during the Laplace transformation, only the leading term of the continuum Green's function (5) is reproduced as $\|x\|\sqrt{s} \to \infty$. Nevertheless, numerical tests show that the large-scale approximation is accurate even for small x, as illustrated in figure 2.

3. Series remainder

To estimate the series remainder in equation (4), it is convenient to introduce the variable q and the function

$$h_x(q) = g_x(s(q)), \quad q = \frac{w}{s+w}, \quad s = w\frac{1-q}{q}. \tag{14}$$

Under the proper choice of w, the path expansion coefficients are positive, and the function $h_x(q)$ is analytic for $|q| < 1$ and has a singularity at $q = 1$. In what follows, we assume that w satisfies the above conditions. For example, $w = 2d$ for the hypercubic lattice and 8 for the triangular one. Now, series (4) can be written as

$$h_x(q) = \sum_{n=0}^{\infty} c_{x;n} q^{n+1+|x|}, \quad c_{x;n} = \frac{N_x(n)}{w^{n+1+|x|}}, \tag{15}$$

and the remainder is defined as

$$R_{x;n}(q) = \sum_{k=n}^{\infty} c_{x;k} q^{k+1+|x|}. \tag{16}$$

To estimate R, we approximate the path expansion coefficients $c_{x;n}$ and then sum up the result.

From the Fourier integral (2) it follows that

$$c_{x;n} = \frac{1}{w(2\pi)^d} \int \cdots \int_{-\pi}^{\pi} \left(1 + \frac{S(k)}{w}\right)^{n+|x|} \mathrm{e}^{-\mathrm{i}kx}\, \mathrm{d}k. \tag{17}$$

For a large n and small S, the power function in the integrand can be approximated by the exponent $(1 + S/w)^{n'} \approx \mathrm{e}^{tS}$, where $t = (n' + \varepsilon)/w$ and ε is a fitting parameter such that $\varepsilon = 0$ corresponds to the upper boundary. If $w > -\min_k S(k)$ then the maximum of $S(k)$ makes a dominant contribution to the Fourier integral. However, for some lattices such as hypercubic, the convenient choice of w might include k-points with $w = -\min_k S(k)$, so their contributions should also be taken into account. In all cases, the path expansion coefficients can be approximated by the propagator as follows:

$$c_{x;n} \approx \frac{\sigma_n}{w} \tilde{g}_x\left(\frac{n + \varepsilon + |x|}{w}\right), \tag{18}$$

where σ_n accounts for the symmetry. For example, for bipartite lattices, if w is half-bandwidth, then $\sigma_{2n} = 2$ and $\sigma_{2n+1} = 0$. Numerical tests show that this approximation is accurate over a broad range of n including the maximum of $c_{x;n}$, as demonstrated in figure 3.

The estimate (18) gives too complicated series even if the continuum propagator (7) is used. A possible workaround is to approximate the latter by a 'summable' function:

$$\tilde{g}^{\mathrm{lat}}(t,x) = \frac{V_1}{(4\pi Dt)^{d/2}} \exp\left(-\frac{\|x\|^2}{4Dt}\right) \lesssim V_1 \left(\frac{w}{4\pi D}\right)^{d/2} \left(wt + \frac{w}{2dD}\|x\|^2\right)^{-d/2} \tag{19}$$

resulting in

$$c_{x;n} \approx \frac{\sigma_n V_1}{w} \left(\frac{w}{4\pi D}\right)^{d/2} \left(n + \varepsilon + |x| + \frac{w}{2dD}\|x\|^2\right)^{-d/2}, \tag{20}$$

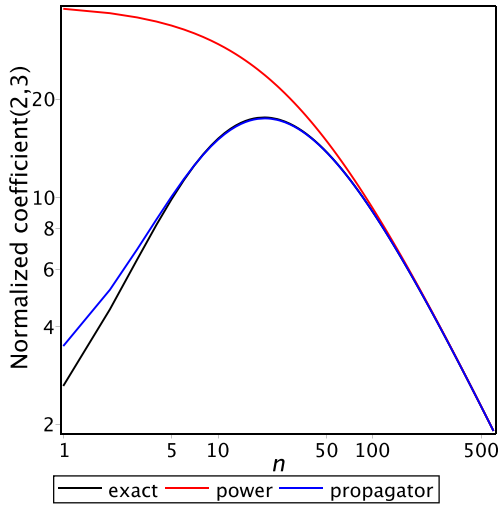

Figure 3. Two approximations of path expansion coefficients $c_{x;n}$ for triangular lattice at $x = (2,3)$.

which is still accurate if

$$n + |x| \gg \frac{w}{2dD}\|x\|^2, \tag{21}$$

and provides the upper boundary otherwise, see figure 3. Now equation (16) can be summed up explicitly, resulting in

$$R_{x;n}(q) \approx R^{\Phi}_{x;n}(q,\varepsilon) \tag{22}$$

where ε is a parameter and the functional form of R^{Φ} depends on σ_n:

$$R^{\Phi}_{x;n}(q,\varepsilon) = \frac{V_1}{w}\left(\frac{w}{4\pi D}\right)^{d/2} q^{n+1+|x|}\ \Phi\left(q, \frac{d}{2}, n+\varepsilon+|x|+\frac{w}{2dD}\|x\|^2\right) \tag{23}$$

for $\sigma_n = 1$ and

$$R^{\Phi}_{x;2n}(q,\varepsilon) = \frac{2V_1}{w}\left(\frac{w}{8\pi D}\right)^{d/2} q^{2n+1+|x|}\ \Phi\left(q^2, \frac{d}{2}, n+\frac{1}{2}\left(\varepsilon+|x|+\frac{w}{2dD}\|x\|^2\right)\right) \tag{24}$$

for $\sigma_{2n} = 2$, $\sigma_{2n+1} = 0$, where $\Phi(q,p,\alpha) = \sum_{n=0}^{\infty}(n+\alpha)^{-p}q^n$ is the Lerch transcendent function. The best estimate is expected for the value of ε corresponding to the large-n asymptotics of the path expansion coefficients, which we denote as ε_∞ (1/2 for the hypercubic lattice and 1/3 for the triangular one). Then a strict upper boundary can be obtained with some $\varepsilon_{\mathrm{up}} \leqslant \varepsilon_\infty$. Numerical tests for the path expansion coefficients show that $\varepsilon_{\mathrm{up}} = \varepsilon_\infty$ for the triangular lattice, whereas for the hypercubic lattice, $\varepsilon_{\mathrm{up}} = 1/4$ for $d \leqslant 6$. A tight lower boundary in the functional form of equation (20) is meaningful only for small x with some $\varepsilon_{\mathrm{low}} > \varepsilon_\infty$, see figure 4. In a general case, the lower boundary is zero.

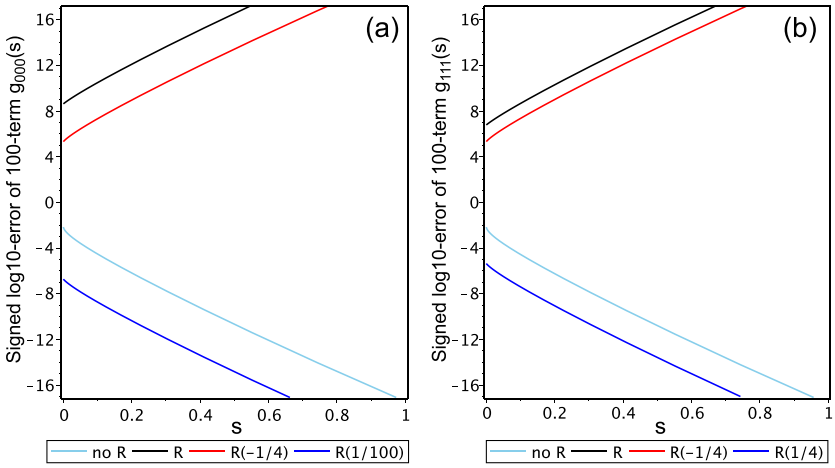

Figure 4. Error in evaluation of LGF for the simple cubic lattice at (a) origin and (b) point $(1,1,1)$ by path expansion with different $\epsilon_{\mathrm{up,low}} - \epsilon_\infty$ (shown in parentheses) in the remainder (24).

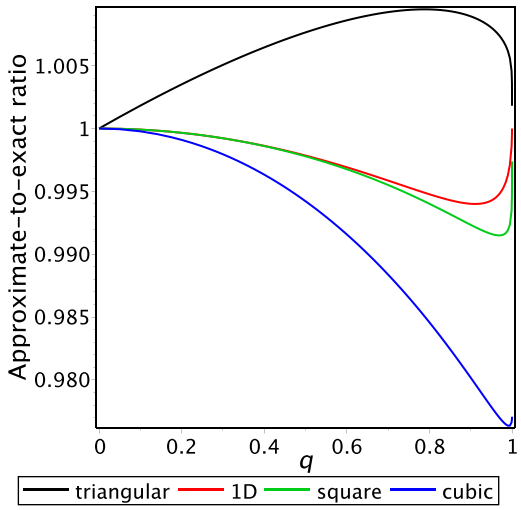

Figure 5. Lerch transcendent approximation to Green's function of several lattices at origin. Here ε is determined by the first path expansion coefficient (e.g. $\varepsilon = 2^{2/d}d/2\pi$ for hypercubic lattices).

By taking $n=0$ in equation (23), we obtain an approximation of the LGF itself:

$$h_x(q) \approx R^{\Phi}_{x;0}(q,\varepsilon)\,, \tag{25}$$

where ε should be determined by some fitting procedure. The simplest fitting is by the first path expansion coefficient, yielding a few-percent accuracy for the LGF at the origin (figure 5).

4. Recurrence relations

The Laplace equation itself cannot provide a platform for recurrent evaluation of LGF in multiple dimensions. However, there is a hidden space-time symmetry due to translational invariance, which can provide additional identities sufficient to derive one-dimensional recurrence relations. By differentiating the Fourier transform of the propagator $\hat{\tilde{g}}(t,k) = \mathrm{e}^{tS(k)}$ with respect to k_i and then taking the inverse Fourier transform, we obtain d identities for the propagator:

$$-\frac{t}{x_i}\sum_{|z|=1} z_i \tilde{g}_{x+z}(t) = \tilde{g}_x(t), \quad i = 1,\dots,d, \tag{26}$$

or equivalent identities for LGF and its integral:

$$\frac{1}{x_i}\sum_{|z|=1} z_i\, g_{x+z}(s) = -\int_s^\infty g_x(s')\,\mathrm{d}s', \quad i = 1,\dots,d, \tag{27}$$

where it is assumed that $x_i \neq 0$. Importantly, the right-hand side of equation (27) does not depend on i, so that we have $d-1$ identities for the LGF itself:

$$\frac{1}{x_i}\sum_{|z|=1} z_i\, g_{x+z}(s) = \text{const}, \quad i = 1,\dots,d, \tag{28}$$

where the constant does not depend on i (but depends on x and s). Combined with the Laplace equation, they provide the required recurrence relations at least for lattices with low enough coordination number. The easiest recursion is to resolve the LGF plane-by-plane from a given point to the origin. This requires the existence of a plane whose lattice points have no more than d nearest neighbors at one side out of the plane. For the hypercubic lattice, any plane satisfies this condition. For the simplectic honeycomb lattice $\mathbb{A}_d$, including triangular and face-centered cubic lattices, the condition is satisfied by $\mathbb{A}_{d-1}$ plane. For the body-centered cubic lattice, the required plane is (110). The computing path of such recurrences can be determined iteratively through recursive evaluations. Alternatively, it can be optimized to achieve better linear scaling with distance. Usually, such a path has two parts: the first is to the nearest high-symmetry point and then along the high-symmetry direction. The recurrence propagates differences, thus requiring high-precision calculations at large s. It should be noted that known recurrence schemes in two and three dimensions [9, 13] are different from the proposed one but can be derived from it.

Since equation (28) includes only the nearest neighbors, the recurrence basis includes only the origin and its symmetry-unique neighbors. For primitive isotropic lattices, we can write the basis explicitly:

$$g_x = \sum_{n=0}^{d} P_n\, g_n, \quad g_n = g_{e^1+e^2+\ldots+e^n}, \tag{29}$$

where e^i are inversion-unique bond (edge) vectors (for hypercubic lattice they coincide with the translation vectors), P_n are polynomials in $s + w_0$ (or $1/q$), and g_n constitute the basis: the LGF values at the seeding core of the recurrence equation. Here we assume that vectors e^i are chosen such that all the points $e^1 + e^2 + \ldots + e^n$ are inequivalent by symmetry. The basis size is $d+1$ because vectors $e^1,\dots,e^d$ taken with unit coefficients span all points within one unit cell distance from the origin, whereas all other points are reducible to them by equation (29).

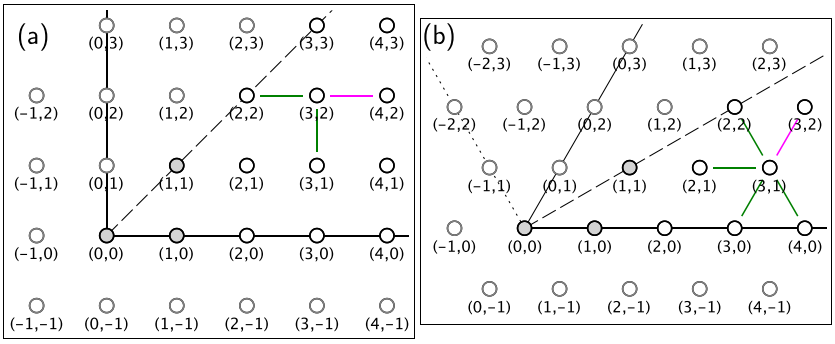

Figure 6. Coordinate systems for (a) square and (b) triangular lattices. The fundamental domain is bounded by the x_1-axis and the dashed line. Recurrence scheme for evaluation of $g_{(4,2)}$ for square lattice and $g_{(3,2)}$ for triangular one are shown by colored bonds. For example, the value of $g_{(4,2)}$ can be obtained from known values of $g_{(3,2)}, g_{(3,1)}, g_{(2,2)}$ by equation (32).

We will explicitly construct recurrence schemes for hypercubic and triangular lattices. For the former, equation (28) reduces to

$$\frac{1}{x_i} D^i g_x = \text{const}, \quad i = 1, \ldots, d, \tag{30}$$

where

$$\left(D^i f\right)_x = f_{x+e^i} - f_{x-e^i}. \tag{31}$$

Using equation (30) we exclude all g_{x+e^i} for $i = 2, \ldots, d$ from the Laplace equations yielding the recurrence

$$g_{x+e^1} = g_{x-e^1} + \frac{x_1}{|x|}\left((s+2d)\, g_x - 2\sum_{i=1}^{d} g_{x-e^i}\right) \tag{32}$$

illustrated in figure 6. The recurrence basis (29) is shown in figure 7 in terms of $h_n(q)$. For the triangular lattice, equation (28) reduces to

$$\frac{\left(D^1 - D^3\right) g_x}{x_1} = \frac{\left(D^2 + D^3\right) g_x}{x_2}, \tag{33}$$

where the three bond vectors are $e^1 = (1,0)$, $e^2 = (0,1)$, $e^3 = (-1,1)$, see figure 6. By excluding g_{x+e_2} from the Laplace equation we obtain the recurrence

$$(x_1 + x_2)\, g_{x+e^1} = (s+6)\, x_1 g_x - (x_1 - x_2)\, g_{x-e^1} - 2x_1 g_{x-e^2} - (2x_1 + x_2)\, g_{x-e^3} + x_2 g_{x+e^3}, \tag{34}$$

which should be propagated across the (11) lattice plane within the fundamental domain, as shown in figure 6.

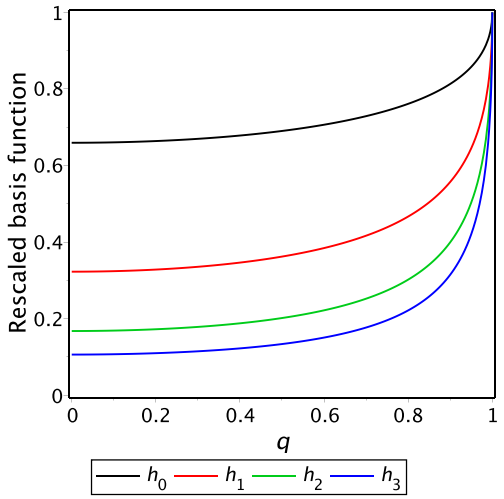

Figure 7. Recurrence basis for the simple cubic lattice. The plotted functions are rescaled as $h_n(q)/h_n(1)/q^{n+1}$.

5. Series at zero

By differentiating equation (27) with respect to s we obtain

$$\frac{1}{x_i}\sum_{|z|=1} z_i\, g'_{x+z} = g_x, \tag{35}$$

which together with equation (29) to exclude non-basis functions produces a set of $d+1$ first-order linear differential equations for $g_0,\dots,g_d$ with the coefficients linear in s. This set is equivalent to a d-order linear differential equation for g_0 with polynomial coefficients in s or q. The reduced order is caused by the algebraic relationship between g_0 and g_1:

$$w_0 g_1 = (s+w_0)\, g_0 - 1. \tag{36}$$

We illustrate this approach for hypercubic LGF. To derive the differential equation, we combine equation (30) written for e^n with the Laplace equation centered at g_n to exclude $g_{e^1+\dots+e^{n-1}+2e^n}$ and obtain the set of equations for $g_n(s)$

$$(s+2d)\, g'_n - 2n g'_{n-1} - 2\,(d-n)\, g'_{n+1} = (n-1)\, g_n, \quad n=0,\dots,d \tag{37}$$

or equivalent set for $h(q)$

$$\mathrm{d}q^{-n}\left(q^{n-1}h_n\right)' = n h'_{n-1} + (d-n)\, h'_{n+1}. \tag{38}$$

The determinant of the tridiagonal matrix at h' is equal to $Q(q)/Q(0)$, where

$$Q(q) = \prod_{k=0}^{[(d-1)/2]} \left(q^2 - q_k^2\right), \text{ and } q_k = \frac{d}{d-2k} \tag{39}$$

are the singularities of hypercubic LGF. The set of first-order equation (38) can be converted into a single high-order equation for h_0:

$$\sum_{n=0}^{d} Q_n(q)\left(q\frac{\mathrm{d}}{\mathrm{d}q}\right)^n h_0(q) = 0, \tag{40}$$

where

$$Q_d = Q,\ Q_{d-1} = dq^4\frac{\mathrm{d}}{\mathrm{d}q^2}\frac{Q(q)}{q^2},\ Q_0 = (-1)^d Q(0), \tag{41}$$

and the rest of Q_n are polynomials of q^2 of the same order as Q.

Compared to the approach of [14], differential equations allow for a more efficient series expansion of LGF at its singularities. We demonstrate this for the hypercubic lattice. All solutions of equation (38) can be obtained as a series for the variable $z = 1 - q^2$ or $p = \sqrt{z}$ [14]:

$$q^{n-1}h_n(q) = A_n\left(p^2\right) + Z(p)B_n\left(p^2\right),\quad Z(p) = p^{d-2}\begin{cases}1 & \text{for odd } d\\ \ln(p_0/p) & \text{for even } d,\end{cases} \tag{42}$$

where $A(z)$ and $B(z)$ are analytic functions for $|z| < 1$ and p_0 is a free parameter that can be conveniently set to $p_0 = 4$ for $d = 2$ and $p_0 = 1$ otherwise. Because h_1 is constrained by equation (36), the set of equation (38) has d linearly independent solutions: $d-1$ regular ($B = 0$) and one singular ($B \neq 0$). The Green's function (42) can now be written as

$$q^{n-1}h_n(q) = \sum_{m=1}^{d} C_m A_{mn}\left(p^2\right) + C_d Z(p)B_{dn}\left(p^2\right) + \delta_{n1}\left(C_1 - \frac{1}{2d}\right), \tag{43}$$

where regular solutions are labeled as A_{mn} with $m = 0,\ldots,d-2$ and the singular one is labeled as A_{dn} and B_{dn}, so that index m enumerates the differential equation basis and n enumerates the recurrence basis. Here the functions $A_{mn}(z)$ are defined as solutions to equation (38) with $A_{m0}(z) = z^m + o(z^{d-2})$, whereas the singular solution is obtained under the conditions $B_{dn}(0) = 1$ and $A_{d0} = o(z^{d-2})$. The series for all $A_{mn}(z)$ and $B_{dn}(z)$ have rational coefficients that can be determined recursively using equation (38). The coefficient C_d at the singular part was derived in [14]. The coefficients at regular solutions are zero in lower dimensions and nontrivial in higher dimensions. They can be expressed in terms of $h_n(1)$ which should be evaluated using another approach. For the simple cubic lattice,

$$C_1 = h_0(1),\quad C_2 = \frac{9h_0(1)}{32} + \frac{3}{64\pi^2 h_0(1)} \tag{44}$$

in consistency with [16]. The accuracy of the series is illustrated in figure 8: it is decreasing faster with distance from the origin compared to the path expansion series. Nevertheless, for any value of the argument, either the path expansion series or series at singularities allows for an efficient LGF evaluation with practically arbitrary precision.

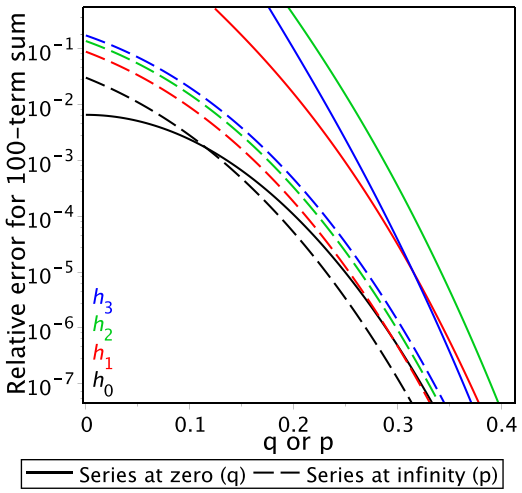

Figure 8. Error in evaluation of h_n functions for simple cubic lattice by two kinds of series without remainder near their convergence boundaries, which are $q=0$ for series in p (series at $s=0$) and $p=0$ for series in q (series at $s=\infty$).

6. Conclusions

The discussed approaches implemented in this work allow for efficient evaluation of LGF for simple lattices at any point of figure 1, that is for any value of coordinates and argument $\Re s \geqslant 0$. This includes approximate, arbitrary-precision, and symbolic computations. The existence of a root-free band dispersion $S(k)$ is the most critical for all methods: for the Fourier integral and large-scale approximation it accelerates computations. For the path expansion series it allows for obtaining explicit formulas for series coefficients and remainder. Recursive evaluation, differential equation, and series at zero are known only for latices with a root-free $S(k)$. The developed two kinds of uniform approximations (large-scale and Lerch transcendent) for fast generic evaluation of LGF show good accuracy for triangular and hypercubic lattices.

Several questions remain open for high-dimensional LGF ($d>3$). First, it is unclear whether recursive evaluation and representation (29) are possible for lattices with a high coordination number such as face- and body-centered hypercubic lattices. Second, we might expect a relationship between coefficients C_m in equation (43) for $d>3$ similar to equation (44) telling that the series at zero of the simple cubic LGF at any lattice point involves only one non-trivial constant: the LGF value at the origin. In addition, the low accuracy of these series near the natural convergence boundary (figure 8) might indicate their non-optimal representation.

Data availability statement

The data that support the findings of this study are openly available at the following URL/DOI: https://cmsos.github.io/lgf/.

Acknowledgments

A Z thanks Denis Andrienko for reviewing the manuscript. The author declares that no competing interests exist.

ORCID iD

Andriy Zhugayevych https://orcid.org/0000-0003-4713-1289

References

[1] Guttmann A 2010 Lattice Green's functions in all dimensions *J. Phys. A: Math. Theor.* A **43** 305205
[2] Berciu M and Cook A 2010 Efficient computation of lattice Green's functions for models with nearest-neighbour hopping *Europhys. Lett.* **92** 40003
[3] Economou E N 2006 *Green's Functions in Quantum Physics* (Springer)
[4] Argyrakis P, Maragakis M, Chumak O and Zhugayevych A 2006 Dynamic correlations in an ordered c(2 × 2) lattice gas *Phys. Rev.* B **74** 035418
[5] Morgan W, Christensen J, Hamilton P, Jorgensen J, Campbell B, Hart G and Forcade R 2020 Generalized regular k-point grid generation on the fly *Comput. Mater. Sci.* **173** 109340
[6] Watson G 1939 Three triple integrals *Q. J. Math.* **10** 266
[7] Zucker I 2011 70+ Years of the Watson Integrals *J. Stat. Phys.* **145** 591
[8] Katsura S and Inawashiro S 1971 Lattice Green's functions for the rectangular and the square lattices at arbitrary points *J. Math. Phys.* **12** 1622
[9] Morita T 1971 Useful procedure for computing the lattice Green's function - square, tetragonal and BCC lattices *J. Math. Phys.* **12** 1744
[10] Horiguchi T 1972 Lattice Green's functions for the triangular and honeycomb lattices *J. Math. Phys.* **13** 1411
[11] Inoue M 1974 Lattice Green's function for the face centered cubic lattice *J. Math. Phys.* **15** 704
[12] Morita T 1975 Use of a recurrence formula in computing the lattice Green function *J. Phys. A: Math. Gen.* A **8** 478
[13] Joyce G 2002 Exact evaluation of the simple cubic lattice Green function for a general lattice point *J. Phys. A: Math. Gen.* A **35** 9811
[14] Joyce G 2003 Singular behaviour of the lattice Green function for the d-dimensional hypercubic lattice *J. Phys. A: Math. Gen.* A **36** 911
[15] Maassarani Z 2000 Series expansions for lattice Green functions *J. Phys. A: Math. Gen.* A **33** 5675
[16] Glasser M and Boersma J 2000 Exact values for the cubic lattice Green functions *J. Phys. A: Math. Gen.* A **33** 5017